CDDpress

www.nature.com/cdd

ARTICLE

Check for updates

BAP1 shapes the bone marrow niche for lymphopoiesis by fine-tuning epigenetic profiles in endosteal mesenchymal stromal cells

Jinguk Jeong[1,2], Inkyung Jung[3], Ji-Hoon Kim[4], Shin Jeon[1,5,7], Do Young Hyeon[1], Hyungyu Min[1,2], Byeonggeun Kang[1,2], Jinwoo Nah[1,2], Daehee Hwang[1], Soo-Jong Um[6], Myunggon Ko[3]✉ and Rho Hyun Seong[1,2]✉

Hematopoiesis occurs within a unique bone marrow (BM) microenvironment, which consists of various niche cells, cytokines, growth factors, and extracellular matrix components. These multiple components directly or indirectly regulate the maintenance and differentiation of hematopoietic stem cells (HSCs). Here we report that BAP1 in BM mesenchymal stromal cells (MSCs) is critical for the maintenance of HSCs and B lymphopoiesis. Mice lacking BAP1 in MSCs show aberrant differentiation of hematopoietic stem and progenitor cells, impaired B lymphoid differentiation, and expansion of myeloid lineages. Mechanistically, BAP1 loss in distinct endosteal MSCs, expressing PRX1 but not LEPR, leads to aberrant expression of genes affiliated with BM niche functions. BAP1 deficiency leads to a reduced expression of pro-hematopoietic factors such as *Scf* caused by increased H2AK119-ub1 and H3K27-me3 levels on the promoter region of these genes. On the other hand, the expression of myelopoiesis stimulating factors including *Csf3* was increased by enriched H3K4-me3 and H3K27-ac levels on their promoter, causing myeloid skewing. Notably, loss of BAP1 substantially blocks B lymphopoiesis and skews the differentiation of hematopoietic precursors toward myeloid lineages in vitro, which is reversed by G-CSF neutralization. Thus, our study uncovers a key role for BAP1 expressed in endosteal MSCs in controlling normal hematopoiesis in mice by modulating expression of various niche factors governing lymphopoiesis and myelopoiesis via histone modifications.

Cell Death & Differentiation (2022) 29:2151–2162; https://doi.org/10.1038/s41418-022-01006-y

INTRODUCTION

Hematopoietic stem cells (HSCs), which exist within the bone marrow (BM) microenvironment, have the capacity to differentiate into all types of blood cells. This microenvironment, termed the "BM niche", is responsible for the self-renewal, differentiation, and migration of HSCs. The niche consists of multiple components, such as various niche cells, cytokines, and extracellular matrix (ECM) components [1–4]. Depending on its anatomical location in the BM, the microenvironment is divided into endosteal niches located near bone lining cells and perivascular niches located near the sinusoid blood vessels [1–4]. Recently, single-cell transcriptome analysis revealed the heterogeneity of the cells consisting the BM niche [5, 6]. However, the specific function of these cells and its underlying molecular mechanisms have yet to be fully uncovered.

BRCA1-associated protein-1 (BAP1) is a deubiquitinating enzyme with ubiquitin C-terminal hydrolase domains, which deubiquitinates monoubiquitinated H2AK119 (H2AK119-ub1) to counteract the functions of polycomb repressor complex 1 (PRC1) [7, 8]. BAP1 has been identified as a tumor suppressor in a variety of malignant and benign tumors in humans [9, 10]. Carriers of germline BAP1 mutations and somatic BAP1 mutations are predisposed to specific tumor types, including mesothelioma, uveal melanoma, and renal cell carcinoma [11–13]. However, the spectrum of tumor susceptibility due to BAP1 mutation differs between humans and mice [14], suggesting that BAP1 may function differently depending on the cell type and species. Functionally, it is well known that BAP1 interacts with transcriptional and epigenetic regulators, including HCF-1, FOXK2, YY1, OGT, and ASXL1/2, to modulate various cellular activities, such as cell cycle, proliferation, metabolism, and differentiation [15–22]. In addition, BAP1 in the endoplasmic reticulum (ER) deubiquitinates and stabilizes the type 3 inositol-1,4,5-triphosphate receptor, which is known to regulate Ca^{2+} release from the ER and activate apoptosis [23]. The roles of BAP1 appear to vary depending on the cell type and context, and further investigation is needed to define the complex functions of BAP1.

Previous studies using various animal models have revealed the crucial role of BAP1 in hematopoiesis. Tamoxifen-induced

[1]School of Biological Sciences, Seoul National University, Seoul 08826, Korea. [2]Institute of Molecular Biology and Genetics, Seoul National University, Seoul 08826, Korea. [3]Department of Biological Sciences, Ulsan National Institute of Science and Technology, Ulsan 44919, Korea. [4]Molecular Recognition Research Center, Korea Institute of Science and Technology, Seoul 02792, Korea. [5]Department of Biological Sciences, University at Buffalo, Buffalo, NY 14260, USA. [6]Department of Integrative Bioscience and Biotechnology, Sejong University, Seoul 05006, Korea. [7]Present address: Department of Systems Pharmacology and Translational Therapeutics, Institute for Immunology, University of Pennsylvania, Philadelphia, PA 19104, USA. ✉email: mgko@unist.ac.kr; rhseong@snu.ac.kr

Edited by M. Piacentini

Received: 9 November 2021 Revised: 7 April 2022 Accepted: 8 April 2022
Published online: 26 April 2022

conditional BAP1 deletion in *Bap1*$^{fl/fl}$creERT2^{+} mice causes a robust expansion of myeloid lineages and features of chronic myelomonocytic leukemia (CMML)-like disease [20]. When BAP1 is systemically deleted, severe defects occur in the development of thymic T cells, peripheral T cell, and BM B cells [24]. Conditional BAP1 deletion in the hematopoietic cells leads to the expansion of myeloid progenitors (MPs) [25]. Recently, B cell-specific deletion of BAP1 in *Mb1*-cre;*Bap1*$^{fl/fl}$ mice results in the depletion of large pre-B cells [26]. These studies have well characterized the hematopoietic cell-intrinsic function of BAP1. However, it remains to be determined whether BAP1 in the BM microenvironment influences the maintenance and differentiation of HSCs.

Here, we show that BAP1 in BM mesenchymal stromal cells (MSCs) plays pivotal roles in regulating hematopoiesis. BAP1 deficiency in distinct endosteal MSCs, expressing PRX1 but not LEPR, impairs the maintenance and differentiation of hematopoietic stem and progenitor cells (HSPCs), favoring myelopoiesis through aberrant expression of genes affiliated with BM niche functions. BAP1 controls the expression of these genes by modulating histone modifications on their promoters. Consistent with in vivo phenotypes, BAP1-deficient MSCs are not capable of supporting B lymphopoiesis and skew the differentiation of HSPCs toward myeloid lineages in vitro. Thus, our findings highlight the importance of BAP1 in endosteal MSCs regulating hematopoiesis in a hematopoietic cell-extrinsic manner.

RESULTS

BAP1 deficiency in BM microenvironment causes loss of HSCs and B cells

To investigate the roles of BAP1 in the BM microenvironment, we crossed *Bap1*$^{fl/fl}$ mice with *Prx1*-cre transgenic mice (Fig. S1A), expressing Cre recombinase in perivascular MSCs, CXCL12-abundant reticular cells, and endosteal MSCs, but not endothelial and hematopoietic cells [27, 28], followed by flow cytometric analyses of overall hematopoiesis in *Prx1*-cre;*Bap1*$^{fl/fl}$ (hereafter, *Bap1* cKO) and *Bap1*$^{fl/fl}$ (hereafter, control) mice. The gating strategy is shown in Fig. S2. In *Bap1* cKO mice, we observed a 2-fold reduction in total BM cell numbers (Fig. S1B). The proportion and cell numbers of LSK cells were also significantly reduced in *Bap1* cKO mice (Fig. 1A and Fig. S1C). Within LSK populations, BAP1 deficiency led to a significant reduction in the proportion and cell numbers of SLAM-enriched HSCs (CD150^{+}CD48^{-} HSCs) as well as LT/ST-HSCs assessed by CD34 and Flt3 markers (Fig. 1B and Fig. S1D).

In addition, the proportion and cell numbers of CLPs and BLPs were severely reduced in *Bap1* cKO mice (Fig. 1C and Fig. S1E). Consistently, *Bap1* cKO mice exhibited reduced proportion and cell numbers of pro-B cells and pre-B cells (Fig. 1D, E and Fig. S1F). Having examined this further, the transition of pro-B cells to pre-B cells was blocked, resulting in the accumulation of pro-B cells. Within the pro-B cell population, we observed developmental arrest during the transition of pre-pro-B cells to early-pro-B cells (Fig. 1F and Fig. S1G). Severe decrease of pre-B cells caused fewer proportion and cell numbers of immature B cells (Fig. 1E and Fig. S1F). There was no significant change in the proportion of circulating mature B cells in the BM of *Bap1* cKO mice (Fig. 1E), but their numbers tended to be slightly reduced, although it did not reach statistical significance (Fig. S1F). The proportion and cell numbers of splenic B cells remained reduced in *Bap1* cKO mice, consistent with the dramatically reduced immature B cells from the BM (Fig. 1G and Fig. S1H, I). Although there were severe defects in B lymphopoiesis in the BAP1-deficient BM, the proportion and cell numbers of MPs were comparable (Fig. 1H and Fig. S1J). Unbalanced hematopoiesis in *Bap1* cKO mice resulted in a decreased proportion of B cell population and an increased proportion of myeloid cell population in the BM (Fig. 1I). As a result, the ratio of B cells to myeloid cells was skewed towards myeloid cells in the BAP1-deficient BM niche (Fig. 1J). Together, these results suggest that BAP1 in the BM microenvironment is essential for HSC maintenance and B cell development.

Hematopoietic defects of *Prx1*-cre;*Bap1*$^{fl/fl}$ mice occur in a cell-extrinsic manner

To explore whether the aberrant hematopoiesis in *Bap1* cKO mice occurs in a hematopoietic cell-extrinsic manner, we adoptively transferred CD45.1^{+} wildtype (WT) LSK cells into busulfan-treated *Bap1* cKO and control mice (Fig. 2A and Fig. S3A). In *Bap1* cKO recipients, we also observed a reduction in numbers of both total BM cells and donor-derived LSK cells (Fig. S3B, C). However, the proportion of LSK cells in *Bap1* cKO recipients were comparable to those of control recipients (Fig. 2B). Similar to the results observed in the primary mice, the development of donor-derived CLPs, pro-B cells, pre-B cells, and immature B cells was severely impaired in *Bap1* cKO recipients (Fig. 2C–F and Fig. S3D–F). Donor-derived immature B cells from the BM of *Bap1* cKO recipients reconstituted the spleen less efficiently than those from control recipients (Fig. S3G). Furthermore, defective B lymphopoiesis in the BM affected the development of donor-derived splenic mature B cells (Fig. 2G and Fig. S3H, I). However, the proportion of donor-derived MPs, especially GMPs and MEPs, was increased in *Bap1* cKO recipients (Fig. 2H and Fig. S3J). Thus, impaired B lymphopoiesis and enhanced myelopoiesis resulted in the myeloid cells-biased BM pool in *Bap1* cKO recipients (Fig. 2I, J). These results indicate that defective hematopoiesis in *Bap1* cKO mice arises from hematopoietic cell-extrinsic effects of the BAP1-deficient BM microenvironment.

Normal hematopoiesis is observed in *Lepr*-cre;*Bap1*$^{fl/fl}$ mice

It is known that almost all Leptin receptor^{+} (LEPR^{+}) perivascular MSCs in the BM express PRX1 [29, 30]. To determine which cell types in the BM microenvironment regulate BAP1-mediated hematopoiesis, we crossed *Bap1*$^{fl/fl}$ mice with *Lepr*-cre transgenic mice expressing cre recombinase in perivascular MSCs. Interestingly, no significant difference in total BM cell numbers and the proportion of CD150^{+}CD48^{-} HSCs, LT-HSCs, and ST-HSCs was observed in *Lepr*-cre;*Bap1*$^{fl/fl}$ (hereafter, *Lepr*-cre;*Bap1* cKO) mice (Fig. S4A, B). In addition, the proportion of CLPs and BLPs was normal in *Lepr*-cre;*Bap1* cKO mice compared to control mice (Fig. S4C). We also detected a normal proportion of BM B cells in *Lepr*-cre;*Bap1* cKO mice (Fig. S4D). There was no difference in the proportion of MPs and the ratio of B cells to myeloid cells in the BM in *Lepr*-cre;*Bap1* cKO mice (Fig. S4E, F).

To isolate LEPR^{+} perivascular MSCs in the BM, we generated *Lepr*-cre;*Bap1*$^{fl/fl}$;*Rosa*-eYFP reporter mice, specifically expressing eYFP in LEPR^{+} perivascular MSCs. We sorted CD45^{-}CD31^{-}TER119^{-}LEPR-eYFP^{+} cells from the enzymatically digested BM in *Lepr*-cre;*Bap1*$^{fl/fl}$;*Rosa*-eYFP mice and confirmed that *Bap1* was deleted in perivascular MSCs (Fig. S4G, H). Next, we confirmed whether the expression of pro-hematopoietic niche factors, including *Scf*, *Cxcl12*, and *Il-7* [29, 31], were changed by BAP1 deficiency. While BAP1 deficiency led to a mild or no decrease in the mRNA expression of *Scf*, *Cxcl12*, *Il-7*, *Vcam1*, and *Angpt1* in LEPR^{+} perivascular MSCs (Fig. S4I), this was not enough to explain the defects in hematopoiesis in vivo. Thus, we postulate that *Bap1* expression in LEPR^{+} perivascular MSCs is dispensable for hematopoiesis.

BAP1 loss in endosteal MSCs suppresses B lymphopoiesis in vitro

Next, we investigated whether BAP1 loss in endosteal MSCs contributed to the severe hematopoietic defects in *Bap1* cKO mice. Flow cytometric analysis revealed that the isolated endosteal MSCs expressed surface markers specific for BM-MSCs, but not for hematopoietic lineage cells (Fig. S5A, B). Using *Prx1*-cre;*Rosa*-eYFP reporting mice, we confirmed that all of endosteal MSCs expressed PRX1 (Fig. 3A). Next, we performed antibody staining to detect the

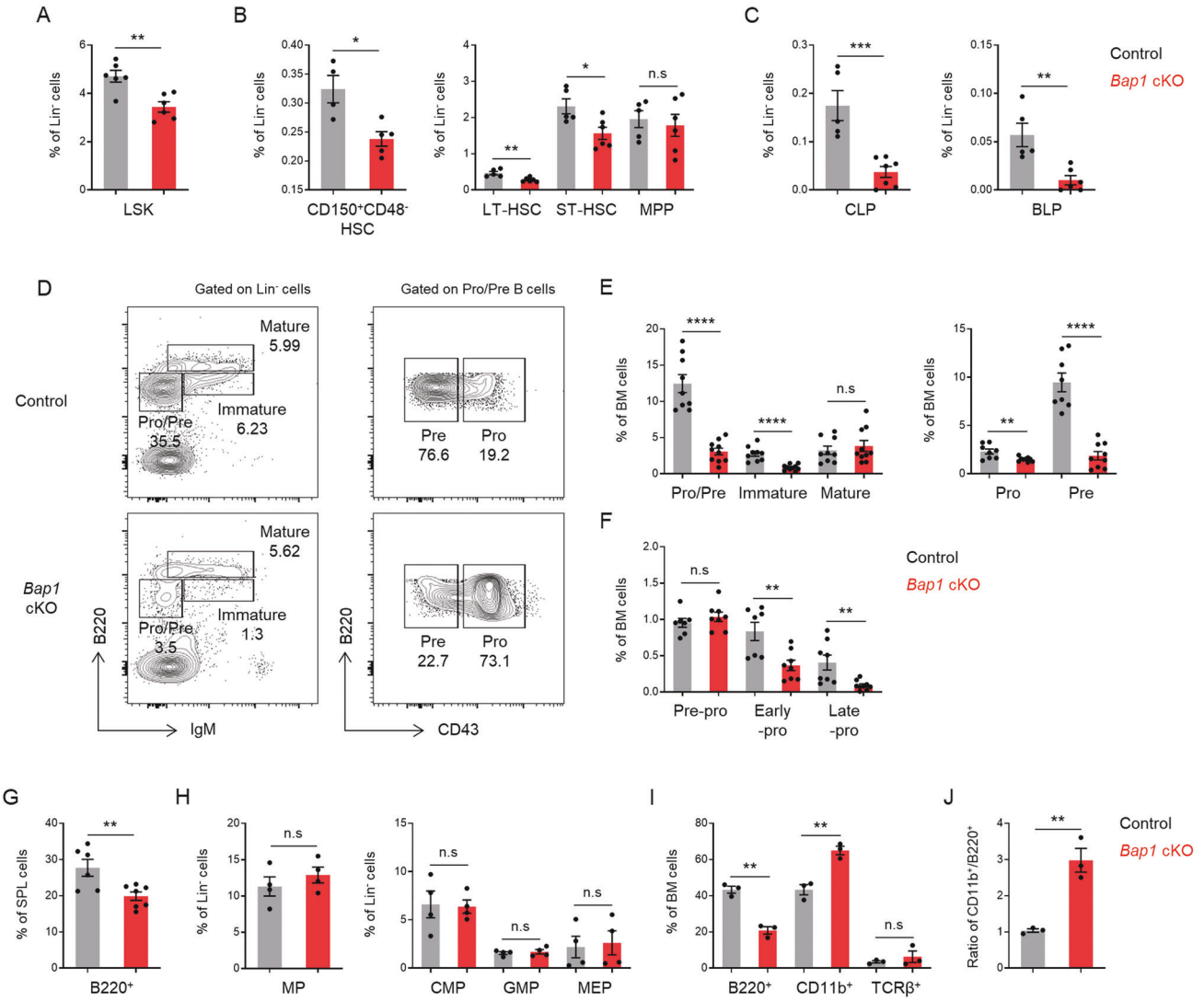

Fig. 1 The proportion of HSCs, lymphoid progenitors, and B Cells is reduced in *Prx1*-cre;*Bap1*$^{fl/fl}$ mice. A–C The proportion of LSK ($Lin^-Sca1^+cKit^+$) cells, CD150$^+$CD48$^-$ HSCs ($Lin^-Sca1^+cKit^+CD150^+CD48^-$), LT-HSCs ($Lin^-Sca1^+cKit^+CD34^-Flt3^-$), ST-HSCs ($Lin^-Sca1^+cKit^+CD34^+Flt3^-$), MPPs ($Lin^-Sca1^+cKit^+CD34^+Flt3^+$), CLPs ($Lin^-Sca1^{low}cKit^{low}IL\text{-}7R\alpha^+Flt3^+$), and BLPs ($Lin^-Sca1^{low}cKit^{low}IL\text{-}7R\alpha^+Flt3^+Ly6D^+$) in the BM of *Bap1* cKO ($n = 5$–7) and control ($n = 4$–6) mice. **D, E** (D) Flow cytometry staining and (E) the proportion of mature B cells (IgM^+B220^{high}), immature B cells (IgM^+B220^+), pre-B cells ($IgM^-B220^+CD43^-$), and pro-B ($IgM^-B220^+CD43^+$) in the BM of *Bap1* cKO ($n = 10$) and control ($n = 9$) mice. **F** The proportion of pre-pro-B cells ($IgM^-B220^+CD43^+CD24^-BP1^-$), early-pro-B cells ($IgM^-B220^+CD43^+CD24^+BP1^-$), and late-pro-B cells ($IgM^-B220^+CD43^+CD24^+BP1^+$) in the BM of *Bap1* cKO ($n = 8$) and control ($n = 7$) mice. **G** The proportion of B220$^+$ cells ($B220^+CD19^+$) in the spleen of *Bap1* cKO ($n = 7$) and control ($n = 6$) mice. **H** The proportion of MPs ($Lin^-Sca1^-cKit^+$), CMPs ($Lin^-Sca1^-cKit^+CD34^+CD16/32^-$), GMPs ($Lin^-Sca1^-Kit^+CD34^+CD16/32^+$) and MEPs ($Lin^-Sca1^-cKit^+CD34^-CD16/32^-$) in the BM of *Bap1* cKO ($n = 4$) and control ($n = 4$) mice. **I** The proportion of B220$^+$ cells, CD11b$^+$ cells, and TCRβ^+ cells in the BM of *Bap1* cKO ($n = 3$) and control ($n = 3$) mice. **J** The ratio of B220$^+$ cells to CD11b$^+$ cells in the BM of *Bap1* cKO ($n = 3$) and control ($n = 3$) mice. All data are mean ± SEM. Statistical analysis was performed using Student's *t*-test. *$p < 0.05$, **$p < 0.01$, ***$p < 0.001$, ****$p < 0.0001$, n.s; not significant ($p > 0.05$).

presence of LEPR. As expected, LEPR was not detected in endosteal MSCs (Fig. 3B). Likewise, we observed little to none *Lepr* mRNA expression in endosteal MSCs as opposed to perivascular MSCs (Fig. 3C). Lastly, we confirmed the complete deletion of BAP1 in endosteal MSCs of *Bap1* cKO mice by qRT-PCR and western blot (Fig. 3D, E). Based on these results, we found that the isolated endosteal MSCs, expressing PRX1 but not LEPR, are a distinct population in the BM.

To analyze HSPC differentiation directly controlled by endosteal MSCs, we established an in vitro co-culture system using endosteal MSCs and WT LSK cells, and assessed hematopoietic differentiation (Fig. 3F). We verified whether endosteal MSCs from control mice could support the differentiation of LSK cells toward B and myeloid lineages (Fig. 3G, H). However, B220$^+$ B cells were barely generated from LSK cells when co-cultured with BAP1-deficient endosteal MSCs, while differentiation toward CD11b$^+$ myeloid lineage cells occurred normally (Fig. 3G, H). Among these myeloid cells, LSK cells seemed to differentiate more preferably into Gr1$^+$CD11b$^+$ cells, relative to CD11c$^+$CD11b$^+$ cells (Fig. 3G, H). These results suggest that the severely impaired B lymphopoiesis seen in *Bap1* cKO mice may be attributable to the loss of BAP1 in endosteal MSCs.

BAP1 in endosteal MSCs regulates genes related to hematopoiesis in the BM

To assess transcriptomic alterations upon BAP1 deficiency in endosteal MSCs, we performed RNA-sequencing (RNA-seq) of

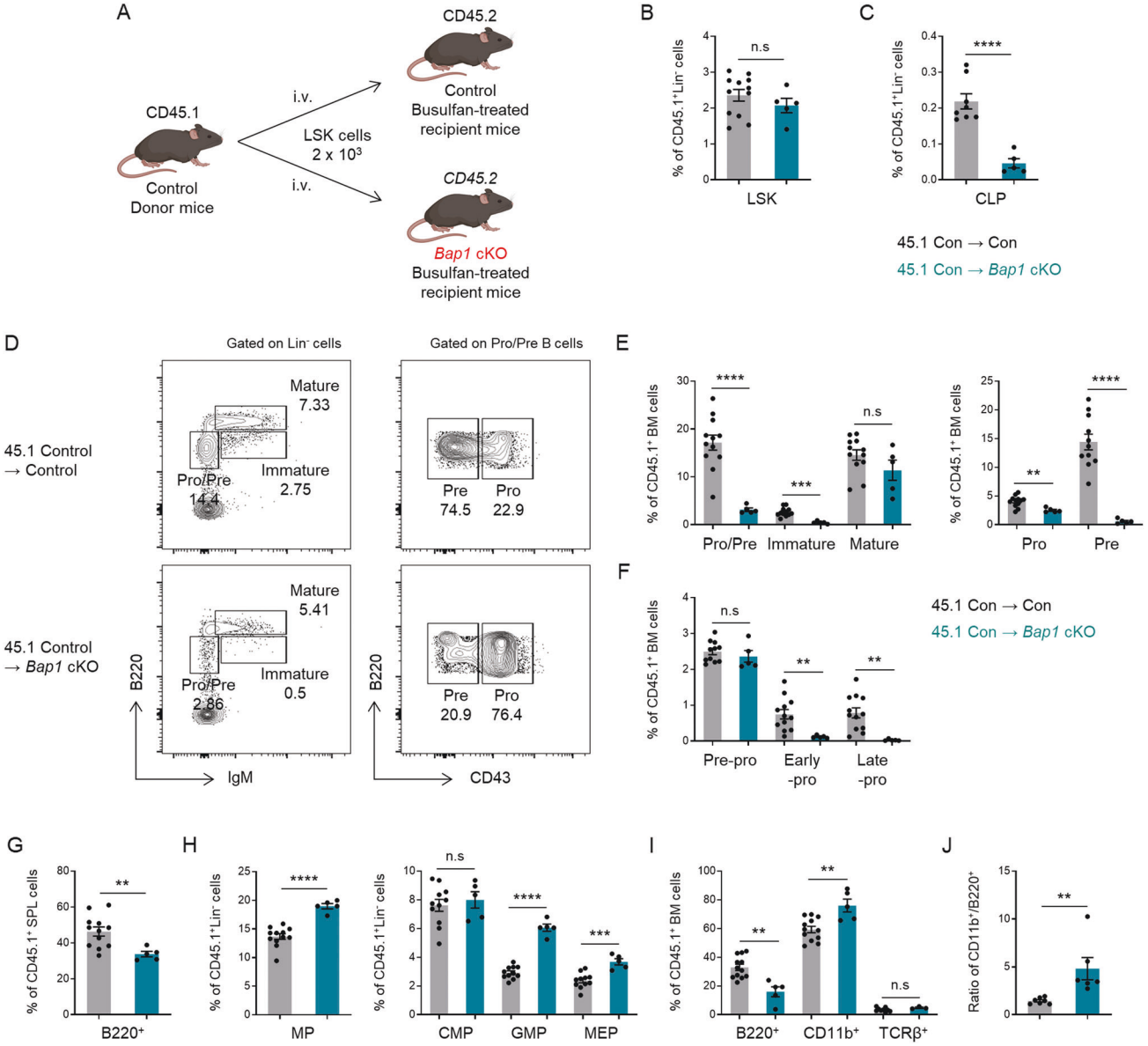

Fig. 2 The phenotype of hematopoiesis in the BAP1-deficient BM niche occurs in a cell-extrinsic manner. A Schematic representation of the BM transplantation. This figure was created with BioRender.com. **B** The proportion of donor-derived LSK cells in the BM of *Bap1* cKO ($n = 5$) and control ($n = 12$) recipients. **C** The proportion of donor-derived CLPs in the BM of *Bap1* cKO ($n = 5$) and control ($n = 8$) recipients. **D**, **E** (D) Flow cytometry staining and (E) the proportion of donor-derived mature B cells, immature B cells, pre-B cells, and pro-B cells in the BM of *Bap1* cKO ($n = 5$) and control ($n = 12$) recipients. **F** The proportion of donor-derived pre-pro-B cells, early-pro-B cells, and late-pro-B cells in the BM of *Bap1* cKO ($n = 5$) and control ($n = 12$) recipients. **G** The proportion of donor-derived $B220^+$ B cells in the spleen of *Bap1* cKO ($n = 5$) and control ($n = 12$) recipients. **H** The proportion of donor-derived MPs, CMPs, GMPs, and MEPs in the BM of *Bap1* cKO ($n = 5$) and control ($n = 12$) recipients. **I** The proportion of donor-derived $B220^+$ cells, $CD11b^+$ cells, and $TCR\beta^+$ cells in the BM of *Bap1* cKO ($n = 5$) and control ($n = 12$) recipients. **J** The ratio of donor-derived $B220^+$ cells to $CD11b^+$ cells in the BM of *Bap1* cKO ($n = 6$) and control ($n = 7$) recipients. All data are mean ± SEM. Statistical analysis was performed using Student's *t*-test. $^{**}p < 0.01$, $^{***}p < 0.001$, $^{****}p < 0.0001$, n.s; not significant ($p > 0.05$).

endosteal MSCs isolated from *Bap1* cKO and control mice. Among differentially expressed genes, 2022 genes were downregulated and 1905 genes were upregulated in BAP1-deficient endosteal MSCs (Fig. 4A). Gene set enrichment analysis (GSEA) showed that genes related to the HSPC niche [32] were significantly enriched among the downregulated genes (Fig. 4B). Furthermore, pro-hematopoietic factors, including *Scf*, *Cxcl12*, *Angpt1*, and *Ebf1*, were downregulated in BAP1-deficient endosteal MSCs (Fig. 4C). Gene ontology (GO) analysis showed that genes downregulated in the BAP1-deficient endosteal MSCs were associated with ECM organization, regulation of cell adhesion and migration (Fig. 4D). We also confirmed that cell adhesion-regulated genes (GO:0045785), including *Vcam1*, *Itga5*, *Lgals1*, and *Spp1*, were significantly reduced (Fig. 4E), and ECM-regulated genes (GO:0062023), including *Col1a1*, *Bgn*, *Mgp*, and *Thbs1*, were remarkably decreased in BAP1-deficient endosteal MSCs (Fig. 4F). Taken together, these results suggest that BAP1 in endosteal MSCs plays key roles in the maintenance of normal HSC niches via transcriptional regulation of diverse niche factors.

Next, we validated the results of RNA-seq by qRT-PCR. As expected, BAP1 deficiency led to severe reduction in the mRNA expression of major pro-hematopoiesis-related genes, such as *Scf*, *Cxcl12*, *Ebf1*, and *Pdgfrb* in endosteal MSCs (Fig. S6A). The mRNA expression of major adhesion and ECM-related genes, including

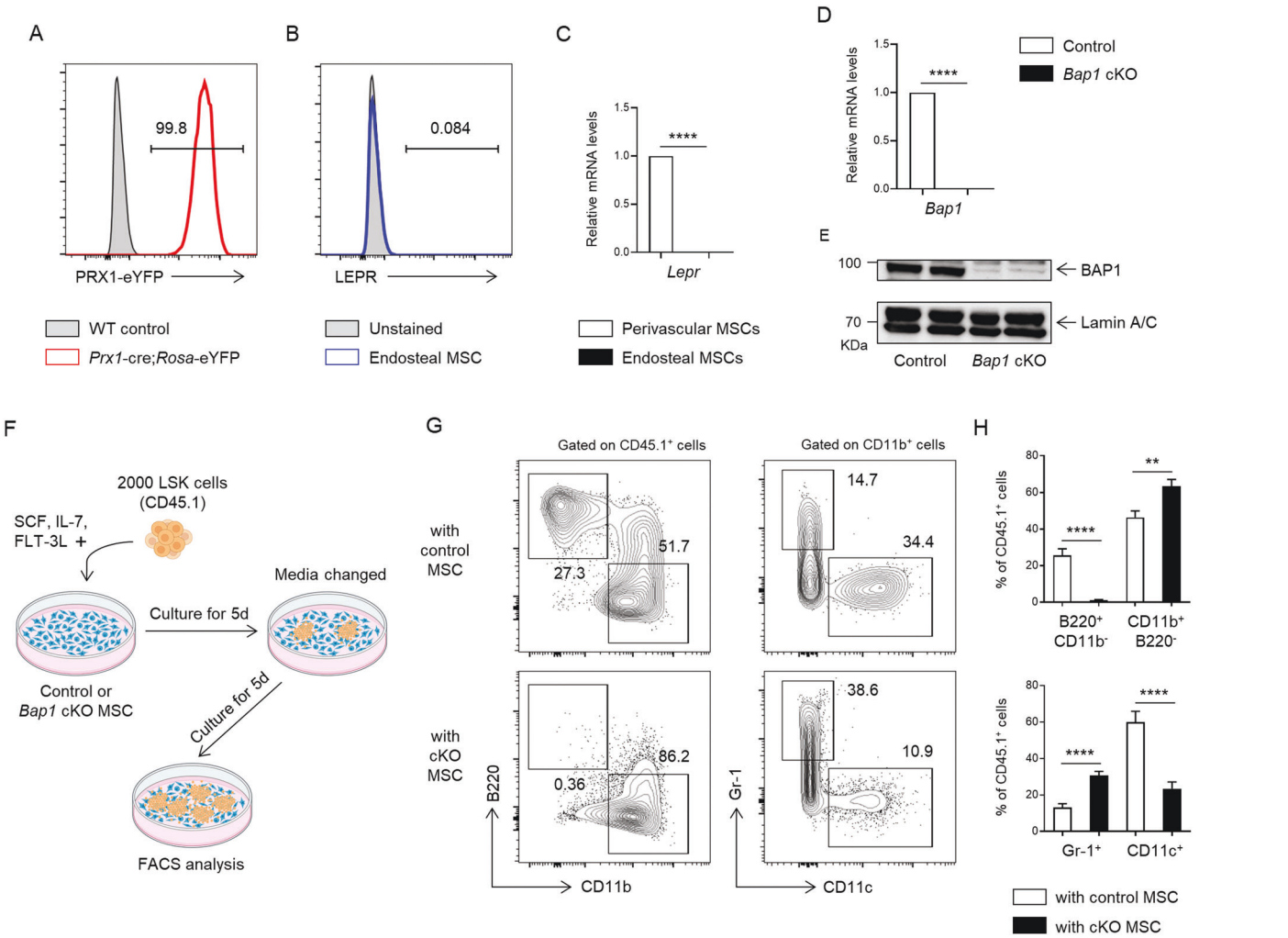

Fig. 3 BAP1 in endosteal MSCs is essential for regulating hematopoiesis. A PRX1-eYFP expression in endosteal MSCs of *Prx1*-cre;*Rosa*-eYFP and WT control mice. **B** Staining with anti-LEPR antibody in endosteal MSCs. **C** *Lepr* relative mRNA levels in endosteal ($n = 3$) and perivascular ($n = 3$) MSCs. **D** *Bap1* relative mRNA levels in endosteal MSCs of *Bap1* cKO ($n = 5$) and control ($n = 5$) mice. **E** BAP1 protein levels of endosteal MSCs of *Bap1* cKO and control mice. **F** Schematic representation of the co-culture experiments of LSK cells and endosteal MSCs. This figure was created with BioRender.com. **G, H** (G) Flow cytometry staining and (H) the proportion of $B220^+CD11b^-$ B cells, $CD11b^+B220^-$ myeloid cells, $CD11b^+Gr\text{-}1^+$ cells, and $CD11b^+CD11c^+$ cells in $CD45.1^+$ cells isolated from co-cultures of LSK cells and endosteal MSCs of *Bap1* cKO ($n = 16$) and control ($n = 14$) mice. All data are mean ± SEM. Statistical analysis was performed using Student's *t*-test. $^{**}p < 0.01$, $^{****}p < 0.0001$.

Col1a1, *Mgp*, *Thbs1*, and *Spp1*, was also decreased (Fig. S6B). On the other hand, the mRNA expression of myelopoiesis stimulating factors *Csf3* (known as *G-csf*) and *C3* were significantly increased in BAP1-deficient endosteal MSCs (Fig. S6C). These data suggest that BAP1 in endosteal MSCs regulates the expression of various genes in distinct ways. Not only does it stimulate lymphopoietic gene expression, but it also represses myelopoietic gene expression.

BAP1 differentially controls the histone modifications of the genes encoding HSC niche factors

BAP1 primarily functions as an H2A deubiquitinase, and regulates gene expression by cooperating with other chromatin modifiers such as PRC1 and PRC2 [7, 8, 25]. As expected, global H2AK119-ub1 levels were increased in BAP1-deficient endosteal MSCs (Fig. S7A). Consistent with previous results [25, 33], BAP1 deletion resulted in an increase in the global levels of H3K27-me3 (Fig. S7B). To dissect the molecular mechanism by which BAP1 controls gene transcription in endosteal MSCs, we investigated whether BAP1 loss affects the histone modifications of genes that are shown to be associated with transcriptional regulation. It has been well documented that trimethylated H3K27 (H3K27-me3) [34] and H2AK119-ub1 [7, 35] on promoters are associated with transcriptional repression. In contrast, the trimethylated H3K4 (H3K4-me3) [36] and acetylated H3K27 (H3K27-ac) [37] have been shown to be associated with transcriptional activation. To examine the occupancy changes in the histone modifications described above, we conducted chromatin immunoprecipitation sequencing (ChIP-seq) analysis on endosteal MSCs of *Bap1* cKO and control mice. We found that the histone activation marks H3K4-me3 and H3K27-ac were remarkably accumulated in upregulated genes in BAP1-deficient endosteal MSCs, consistent with their association with transcriptional upregulation (Fig. 5A). H2AK119-ub1 levels were also increased, but levels of H3K27-me3 were slightly decreased (Fig. 5A). In particular, BAP1 loss led to increased H3K4-me3 and H3K27-ac occupancy without an increase of H3K27-me3 levels on the *Csf3* and *C3* gene regulatory regions, consistent with the dramatic upregulation of these genes (Fig. 5B and Fig. S7C). These results were further validated using ChIP-qPCR (Fig. 5C and Fig. S7D).

Next, we assessed the histone modifications in genes down-regulated in the absence of BAP1. In BAP1-deficient endosteal MSCs, we observed that levels of the repressive H3K27-me3 and

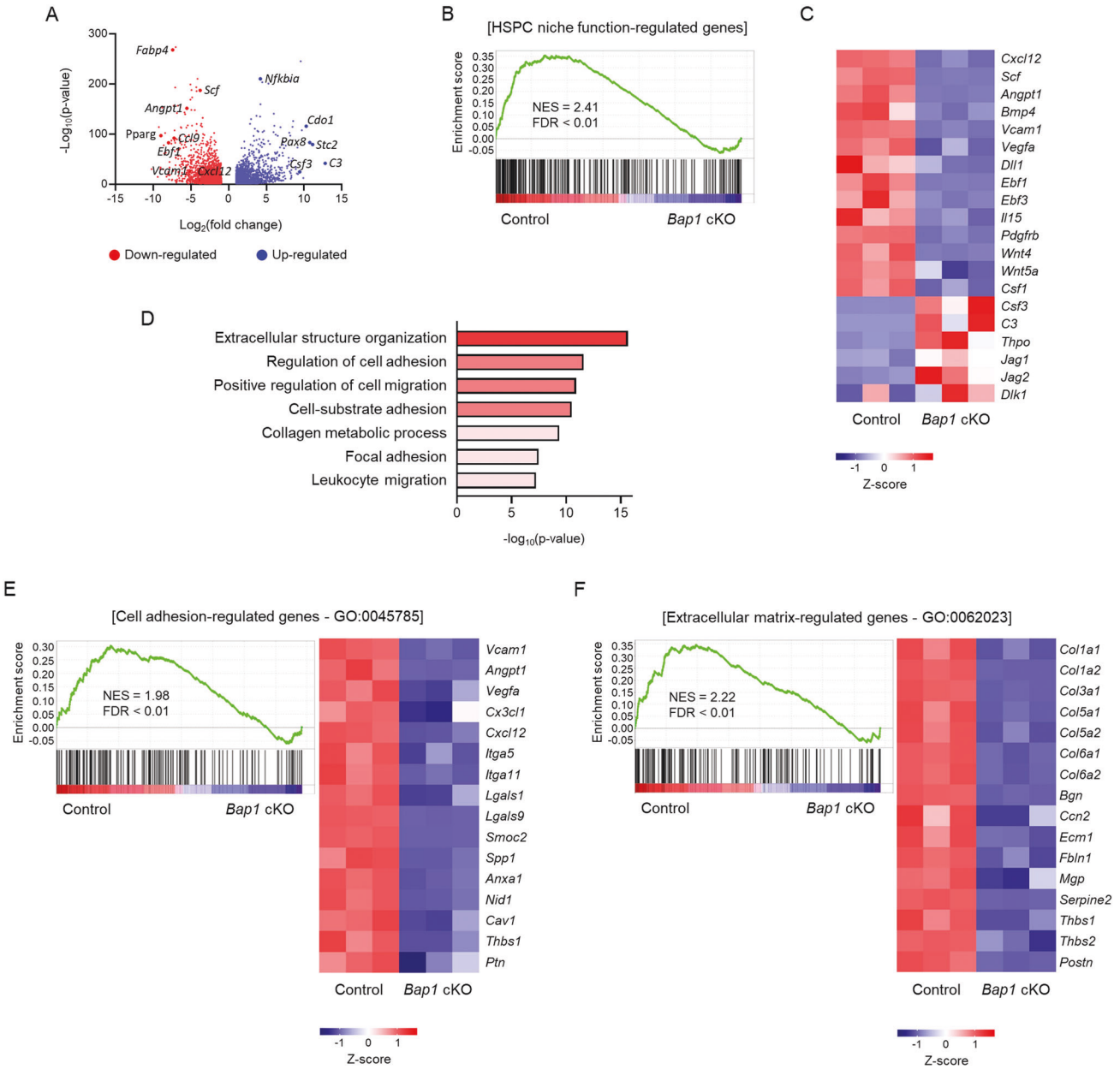

Fig. 4 BAP1-deficient endosteal MSCs show severe defects of the transcriptome related to the hematopoietic niche functions. A Volcano plot of differentially expressed genes in RNA-seq of endosteal MSCs of *Bap1* cKO ($n = 3$) and control ($n = 3$) mice (> 2-fold, $P < 0.05$). Blue dots indicate upregulated genes, and red dots represent downregulated genes in endosteal MSCs of *Bap1* cKO mice. **B, C** (B) GSEA and (C) heat map with gene sets related in hematopoietic stem and progenitor cell niches in endosteal MSCs of *Bap1* cKO ($n = 3$) and control ($n = 3$) mice. **D** GO analysis of downregulated genes in endosteal MSCs of *Bap1* cKO mice. **E, F** GSEA and heat map of (E) cell adhesion-related genes (GO:0045785) and (F) extracellular matrix-related genes (GO:0062023) in endosteal MSCs of *Bap1* cKO ($n = 3$) and control ($n = 3$) mice.

H2AK119-ub1 marks were increased with no significant changes in levels of H3K4-me3 and H3K27-ac, which correlated with the transcriptional repression of these genes (Fig. 5D). For instance, BAP1 deficiency augmented the deposition of H2AK119-ub1 and H3K27-me3 on the *Scf* and *Vcam1* gene regulatory regions in endosteal MSCs, which was further validated using ChIP-qPCR (Fig. 5E, F and Fig. S7E, F). As H3K27-me3 is mediated by EZH2, a representative histone methyltransferase of PRC2 [38], we assessed whether inhibition of H3K27-me3 would exert any effect on gene expression. As expected, pharmacological suppression of EZH2 using GSK126 and GSK343 led to de-repression of *Scf*, *Vcam1*, and *Cxcl12* genes in BAP1-deficient endosteal MSCs (Fig. S7G). Thus, these results suggest that BAP1 in endosteal MSCs fine-tunes hematopoiesis by transcriptionally regulating key niche factors via chromatin modifications.

G-CSF neutralization restores in vitro B lymphopoiesis in the absence of BAP1

To examine whether the observed in vitro B lymphopoiesis defects, shown in Fig. 3G, could be rescued by soluble factors secreted from control endosteal MSCs, we co-cultured WT LSK cells and BAP1-deficient endosteal MSCs in the conditioned medium from control endosteal MSCs. However, the proportion of B cells and myeloid cells was not altered in the presence of cultured medium of control endosteal MSCs (Fig. S8A, B). Then, we asked whether factors secreted from BAP1-deficient endosteal MSCs could

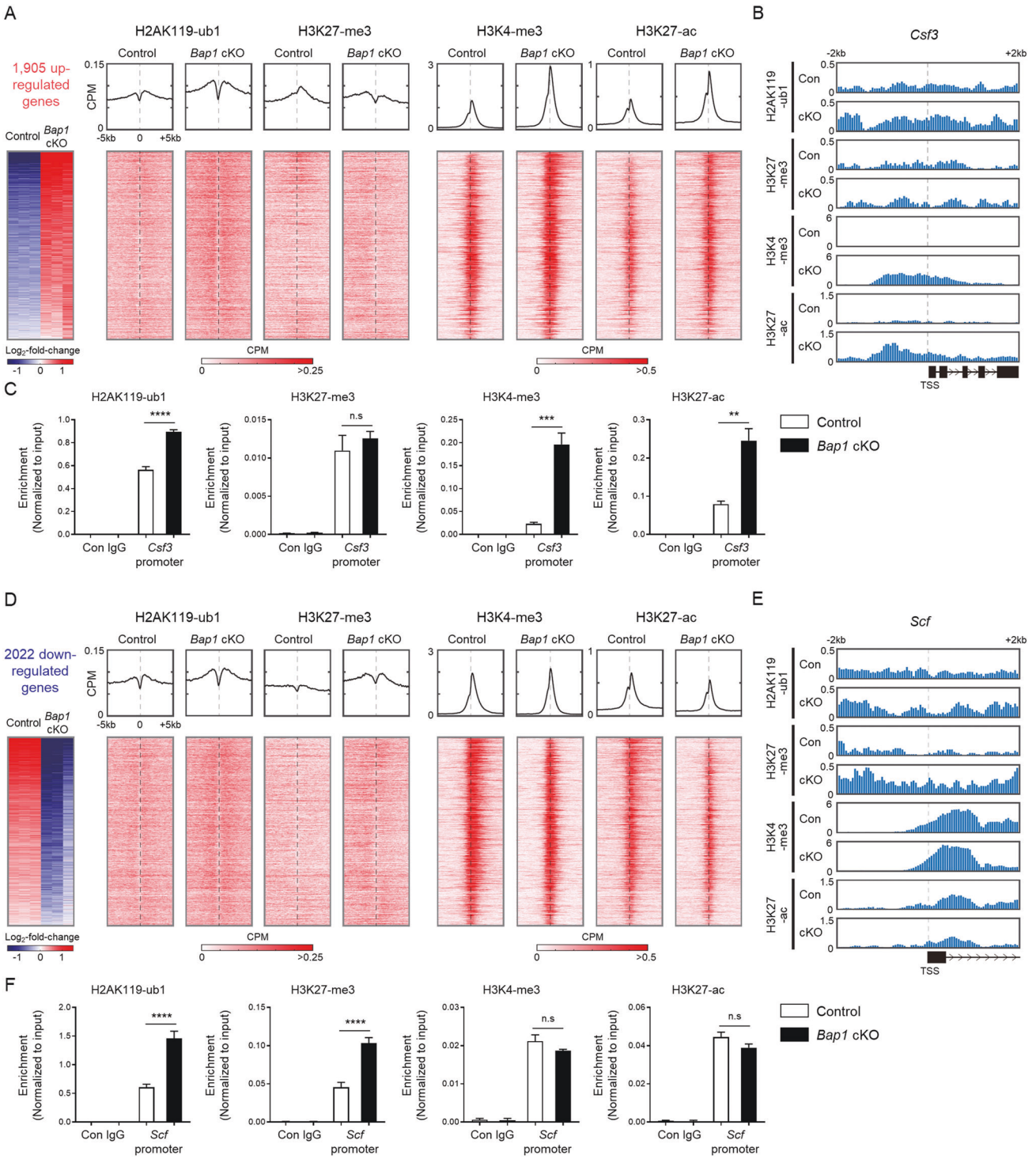

Fig. 5 BAP1 activates lymphopoiesis-related genes expression, whereas it represses myelopoiesis-related gene expression via distinct histone modification. A Heat map showing mRNA expression levels (left) and occupancy distributions of H2AK119-ub1, H3K27-me3, H3K4-me3, and H3K27-ac in the region between transcription start site (TSS)−5kb and TSS+5 kb (right) of genes upregulated in endosteal MSCs of *Bap1* cKO mice compared to control mice. Averaged counts per million (CPM) occupancy profiles are shown above the heat maps. **B** CPM distributions representing occupancy of the indicated marks between the TSS−2kb and TSS+2 kb region of *Csf3* in endosteal MSCs of *Bap1* cKO and control mice. **C** ChIP-qPCR analysis of the indicated marks occupancy on the *Csf3* promoter region in endosteal MSCs of *Bap1* cKO ($n = 6$) and control ($n = 6$) mice. **D** ChIP-seq analysis, as shown in **A**, of genes downregulated in endosteal MSCs of *Bap1* cKO mice compared to control mice. **E** CPM distributions representing occupancy of the indicated marks between the TSS−2kb and TSS+2 kb region of *Scf* in endosteal MSCs of *Bap1* cKO and control mice. **F** ChIP-qPCR analysis of the indicated marks occupancy on the *Scf* promoter region in endosteal MSCs of *Bap1* cKO ($n = 6$) and control ($n = 6$) mice. All data are mean ± SEM. Statistical analysis was performed using Student's *t*-test. $^{**}p < 0.01$, $^{***}p < 0.001$, $^{****}p < 0.0001$, n.s; not significant ($p > 0.05$).

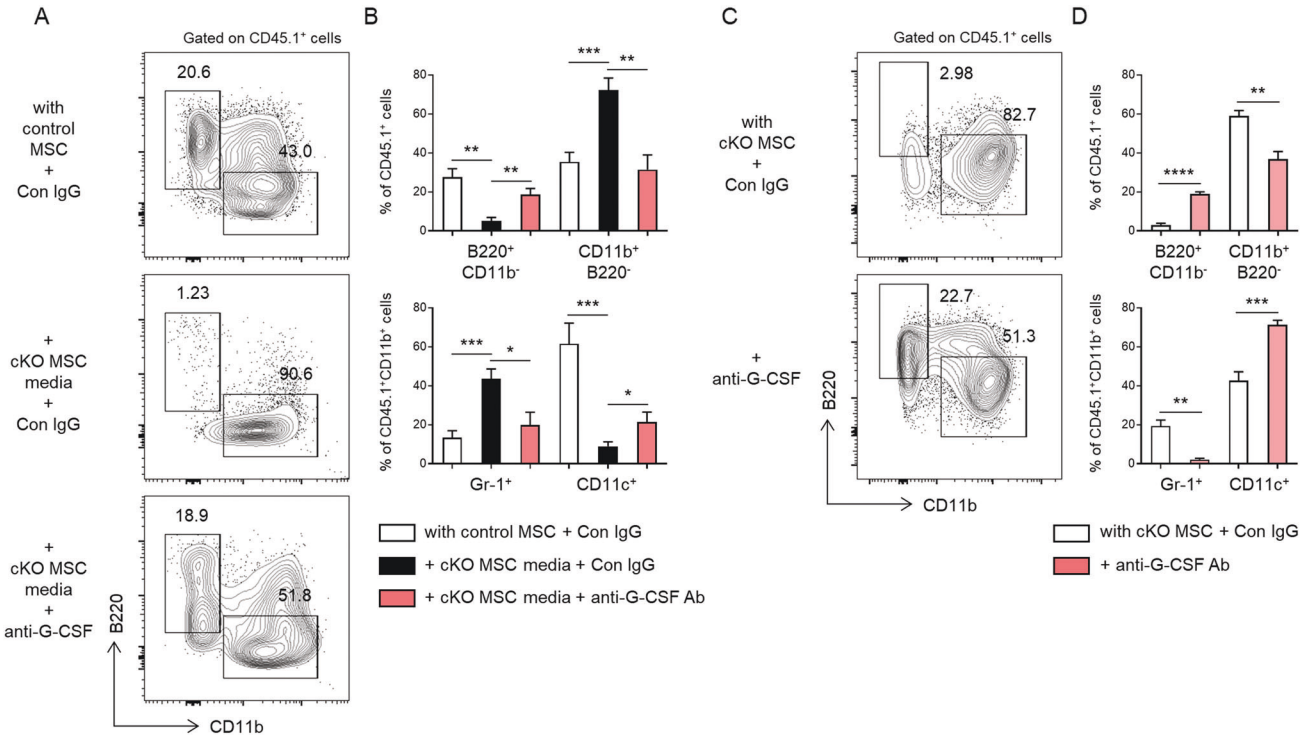

Fig. 6 Impaired B lymphopoiesis in BAP1-deficient conditions is rescued by G-CSF neutralization. A, B (A) Flow cytometry staining and (B) the proportion of $B220^+CD11b^-$ cells, $CD11b^+B220^-$ cells, $CD11b^+Gr\text{-}1^+$ cells, and $CD11b^+CD11c^+$ cells in $CD45.1^+$ cells isolated from co-cultures of LSK cells and endosteal MSCs of control mice in the conditioned medium of endosteal MSCs of *Bap1* cKO mice in the presence ($n = 5$) or absence ($n = 5$) of anti-G-CSF antibody. **C, D** (C) Flow cytometry staining and (D) the proportion of $B220^+CD11b^-$ cells, $CD11b^+B220^-$ cells, $CD11b^+Gr\text{-}1^+$ cells, and $CD11b^+CD11c^+$ cells in $CD45.1^+$ cells isolated from co-cultures of LSK cells and endosteal MSC of *Bap1* cKO mice in the presence ($n = 8$) or absence ($n = 10$) of anti-G-CSF antibody. All data are mean ± SEM. Statistical analysis was performed using Student's *t*-test. $^*p < 0.05$, $^{**}p < 0.01$, $^{***}p < 0.001$, $^{****}p < 0.0001$.

influence hematopoietic differentiation in vitro. To test this, we co-cultured WT LSK cells and control endosteal MSCs in the conditioned medium from BAP1-deficient endosteal MSCs. Strikingly, hematopoietic differentiation from LSK cells was substantially biased toward myeloid lineages, with severe impairment of B lymphopoiesis (Fig. 6A, B)

As *Csf3* gene encoding pro-myelopoietic factor G-CSF was highly upregulated in BAP1-deficient endosteal MSCs shown through RNA-seq and qRT-PCR (Fig. 4C and Fig. S6C), we next examined whether excessive secretion of G-CSF from BAP1-deficient MSCs could antagonize B lymphopoiesis in vitro. To test this, WT LSK cells were co-cultured with control endosteal MSCs in the conditioned medium from BAP1-deficient endosteal MSCs in the presence of anti-G-CSF neutralizing antibody. As shown in Fig. 6A, B, supplementation of anti-G-CSF antibody potently rescued the B lymphopoietic defects. Among differentiated myeloid cells, $CD11c^+CD11b^+$ cells were more pronounced, compared to the $Gr1^+CD11b^+$ cells (Fig. 6B). Likewise, WT LSK cells could also normally differentiate into B cells when co-cultured with BAP1-deficient endosteal MSCs in the presence of anti-G-CSF antibody (Fig. 6C, D). Together, these data suggest that BAP1 in endosteal MSCs prevents excessive secretion of soluble factors including G-CSF, which promotes myelopoiesis but antagonizes B lymphopoiesis to maintain balanced differentiation of hematopoietic precursors in vitro.

DISCUSSION

In this study, we demonstrate that BAP1 in endosteal MSCs is indispensable for the regulation of hematopoiesis. A previous study showed that tamoxifen-induced systemic deletion of BAP1 in $Bap1^{fl/fl}$creERT2$^+$ mice leads to impaired proliferation and survival of CLPs, resulting in aberrant B cell development [24]. Compared with B cell-specific deletion of BAP1 in *Mb1*-cre;$Bap1^{fl/fl}$ mice [26], more severe defects were observed in B cell development when BAP1 was systemically deleted. By disrupting BAP1 in MSCs using *Prx1*-Cre transgenic mice, we show that HSC maintenance and B cell development are significantly impaired. BAP1 deficiency in MSCs caused the suppression of key pro-hematopoietic factors such as *Scf* and *Cxcl12*. In addition, it has been shown that MPs and mature myeloid cells were remarkably expanded in tamoxifen-treated $Bap1^{fl/fl}$creERT2$^+$ mice, causing the CMML-like phenotypes [20]. Another study also showed that hematopoietic cell-specific BAP1 ablation caused myeloproliferative disease (MPD) in mice, indicating hematopoietic cell-intrinsic functions of BAP1 [25]. Our data show that mice with BM niche-specific deletion of BAP1 also display similar phenotypes, including augmented myelopoiesis. Especially, BAP1-deficient MSCs strongly skewed the differentiation of HSPCs toward myeloid lineages in vitro while it potently blocked B lymphopoiesis. Thus, BAP1-deficient MSCs may antagonize B lymphopoiesis, presumably due to excessive secretion of G-CSF in the BM microenvironment. Taken together, these results indicate that BAP1 controls HSC differentiation in both hematopoietic cell-intrinsic and -extrinsic manners.

Although there were severe defects in early B lymphopoiesis in the BM of *Bap1* cKO mice, we detected that the proportion of circulating mature B cells in the BM was not significantly affected. Immature B cells leave the BM and move to the spleen for their maturation [39]. Since PRX1-mediated BAP1 deficiency does not occur in the peripheral microenvironment, such as the spleen, in *Bap1* cKO mice [27], it appears that immature B cells leaving the BM complete their maturation and expansion normally. Because the splenic niche, in which B cell expansion occurs, is not affected

by deleting BAP1 in *Bap1* cKO mice, it is likely that these immature B cells may have had more room to expand during the development process. This may have resulted in a lesser reduction of mature B cells in the spleen than that of immature B cells in the BM. As these circulating mature B cells are thought to return to the BM after completing their maturation in the peripheries [39, 40], this appears to contribute to the slight difference observed in the proportion of mature B cells in the BM. This suggests that B lymphopoiesis in *Bap1* cKO mice is impaired due to the BAP1-deficient BM microenvironment.

When we assessed the effect of BAP1 loss in either $LEPR^{+}$ perivascular MSCs or $PRX1^{+}LEPR^{-}$ endosteal MSCs, BAP1 deficiency slightly reduced *Scf* and *Cxcl12* expression in $LEPR^{+}$ perivascular MSCs, while gene expression changes were more pronounced in $PRX1^{+}LEPR^{-}$ endosteal MSCs. Global transcriptome analysis using endosteal MSCs showed that pro-hematopoietic factors, cell adhesion, and ECM-related genes were positively regulated by BAP1. In particular, *Scf* and *Cxcl12* levels were significantly reduced in BAP1-deficient endosteal MSCs. Since CXCL12 and CXCR4 interaction is essential for HSC homing to BM and overall B lymphopoiesis, CXCL12 deficiency results in severe defects in HSC maintenance and retention of pro-B cells and pre-B cells [28, 41]. In addition, SCF secreted from the BM niche cells is needed to maintain HSCs [42, 43]. Thus, the reduction of *Scf* and *Cxcl12* upon BAP1 deficiency may contribute to the severe defects in HSC maintenance and pre-B cell transition. Moreover, cell adhesion-affiliated molecules, including VCAM1, ANGPT1, and SPP1, are indispensable for the modulation of quiescence and differentiation potentials of HSPCs [44–48]. Furthermore, ECM organization through collagen and fibronectin is an important factor that supports the adhesion of HSCs to the BM microenvironment [49, 50]. Therefore, BAP1 may also influence the interactions between HSCs and the BM microenvironment by activating the cell adhesion and ECM-related gene expression. On the other hand, BAP1 suppresses *Csf3* expression in endosteal MSCs. G-CSF plays an important role in activating neutrophil differentiation and HSC egression from the BM to the blood [51, 52]. We showed that BAP1-deficient endosteal MSCs failed to support B lymphopoiesis in vitro. These defects were rescued by neutralizing G-CSF. Thus, in an in vivo BAP1-deficient environment, both the reduction of pro-hematopoietic factors and an increase in G-CSF may result in severe defects in hematopoiesis.

Upon BAP1 deletion in endosteal MSCs, we demonstrated that global H2AK119-ub1 levels were increased, particularly on promoter regions of genes including *Scf* and *Cxcl12*. It is generally known that gene silencing mediated by the accumulation of H2AK119-ub1 is accompanied by EZH2/PRC2-induced H3K27-me3 [53]. We also showed that H3K27-me3 levels were increased on the same promoter regions where H2AK119-ub1 levels were enriched. This suggests that the increase in H2AK119-ub1 by BAP1 deficiency precedes the increase in H3K27-me3, resulting in gene repression via chromatin condensation. To support this, we confirmed that the reduced *Scf*, *Vcam1*, and *Cxcl12* expression levels were de-repressed by EZH2 inhibition. Thus, BAP1 in endosteal MSCs stimulated the expression of pro-hematopoietic genes, including *Scf*, *Vcam1*, and *Cxcl12*, by suppressing EZH2-mediated PRC2 activity. By contrast, H3K27-me3 levels were not altered on the *Csf3* gene loci where H2AK119-ub1 levels were enriched in the absence of BAP1. Rather, there was a significant increase in the histone activation marks H3K4-me3 and H3K27-ac on the *Csf3* promoter regions. Until now, BAP1's function as a transcriptional repressor rather than an activator was relatively uncommon. It is known that BAP1 represses the expression of cysteine transporter SLC7A11 in an H2A deubiquitinating activity dependent manner, which promotes ferroptosis in tumors [54]. However, the molecular mechanism as to how BAP1 represses gene expression remains unclear. A different study suggests that there is a slight overlap between genes upregulated upon BAP1 deficiency and genes regulated by EZH2 and RING1B [8]. Also, H3K27-me3 levels are not altered on the 5' end of upregulated genes, but rather H3K4-me3 levels are increased [8]. Similar histone modification patterns of *Csf3* promoter regions are shown upon the loss of BAP1. Thus, BAP1 may also be implicated in gene repression independently of EZH2/PRC2-mediated silencing.

In humans, germline and somatic BAP1 mutations are associated with a higher incidence of mesothelioma and uveal melanoma [9–11, 13]. However, $Bap1^{+/-}$ mice and mice carrying germline BAP1 mutations spontaneously develop a spectrum of tumors different from the types observed in humans, including ovarian sex cord-stromal tumors [14]. Systemic deletion of BAP1 in adult mice causes CMML or MPD, but these tumors are not observed in humans with BAP1 mutations [20]. Although BAP1 functions as a tumor suppressor in both humans and mice, there may be differences in the type of cells affected by BAP1 mutation between the two species. The heterogeneity of MSCs in humans remains elusive, and MSCs between humans and mice can be functionally diverse [55]. Thus, further verification is needed to apply our findings regarding BAP1 function in mouse MSCs to their human counterparts.

Taken together, we show that BAP1 in the BM microenvironment is essential for the maintenance of HSCs and B lymphopoiesis by activating the pro-hematopoietic gene expression. It also inhibits expansion of myeloid cells by repressing G-CSF expression via epigenetic modulation. Thus, these findings establish BAP1 as an essential chromatin modulator regulating hematopoiesis in a hematopoietic cell-extrinsic manner.

MATERIALS AND METHODS

Mice

$Bap1^{fl/fl}$ mice were generated from ES cell line (HEPD0526_2_G01) provided by EUCCOM (the Gene-trap consortium) [56]. The strain was crossed with flippase (Flp) transgenic mice to remove the neo cassette. The detailed scheme for the generation of $Bap1^{fl/fl}$ mice is explained in Fig. S1A. *Prx1*-Cre (005584), *Lepr*-Cre (008320), *Rosa*-YFP (006148) transgenic mice, and CD45.1 congenic (002014) mice were obtained from The Jackson Laboratories. All mice were backcrossed into a C57BL/6J background and bred in specific pathogen-free barrier facilities at Seoul National University and Institute of Molecular Biology and Genetics, and were handled according to the protocols of the Institutional Animal Care and Use Committee (IACUC) at Seoul National University.

BM transplantation

To condition the recipient mice (8–10 weeks old) prior to BM adoptive transplantation, the mice were treated 20 mg/kg of busulfan (Sigma Aldrich, B2635) once every day for 3 days via an intraperitoneal injection. Twenty-four hours after the last injection, donor-derived 2000 LSK cells ($Lin^{-}Sca1^{+}cKit^{+}$) were delivered intravenously into the busulfan-treated recipient mice. Mice were analyzed 10 weeks after transplantation (Fig. S3A). Donor and recipient mice were distinguished by the CD45.1/CD45.2 congenic mouse system.

Flow cytometry

BM cells and spleen cells were resuspended by passing through the 70μm cell strainer. To remove the red blood cells, ACK lysis buffer was treated to the cells. The cells were washed with PBS and stained with antibodies for flow cytometric analysis. For HSCs and progenitor cells analysis, anti-Sca1 (D7), anti-c-KIT (2B8), anti-CD150 (9D1), anti-CD48 (HM48-1), anti-CD34 (RAM34), anti-FLT3 (A2F10.1), and a lineage marker cocktail of biotinylated anti-CD3e/anti-CD11b/anti-CD45R/anti-Gr-1/anti-TER119 antibodies were used. For CLPs and BLPs analysis, anti-CD127 (A7R34), and anti-LY6D (49-H4) antibodies were used. For B cell subsets analysis, anti-CD45R (RA3-6B2), anti-IgM (R6-60.2), anti-CD43 (S7), anti-CD24 (M1/69), anti-BP1 (6C3), anti-CD19 (1D3), anti-CD21 (7G6), and anti-CD23 (B3B4) antibodies were used. For myeloid progenitor cells and myeloid cells analysis, anti-CD16/32 [93], anti-CD11b (M1/70), anti-CD11c (HL3), and anti-Gr1 (RB6-8C5) antibodies were used. For MSC characterization analysis, anti-CD31 (MEC13.3), anti-CD45 (30-F11), anti-CD44 (IM7), anti-CD51 (RMV-7), anti-CD29 (HMβ1-1), anti-CD73 (TY/11.8), anti-CD105 (MJ7/18), anti-TCRβ (H57-597), and anti-LepR (R&D) antibodies were used. For isotype control staining, Rat-IgG1.κ

(RTK2071), Rat-IgG2a.κ (RTK2758), Rat-IgG2b.κ (RTK4530), and American hamster-IgG (HTK888) were used. Flow cytometric analysis was performed using FACS Canto II (BD Bioscience). All FACS data were analyzed using FlowJo software. Original FACS plots were included in the Supplementary Material.

Isolation of MSCs

Murine compact bones (femora and tibia) were dissected from the body. Skins, muscles, and tendons were removed by micro dissecting scissors and forceps. After cutting the epiphysis of bones, BM cells were flushed out with α-MEM medium (10% FCS, 1% penicillin–streptomycin) using a 25 g needle and syringe. The flushed bones were cut into 1–2 mm^3 chips. Collected BM cells and bone chips were stored in ice with α-MEM medium (10% FCS, 1% penicillin–streptomycin).

For isolation of *Lepr*-cre;*Rosa*-eYFP$^+$ perivascular MSCs, collected BM cells were digested with Collagenase II (3 mg ml^{-1}), Dispase II (4 mg ml^{-1}), and DNase I (0.1 mg ml^{-1}) at 37 °C on 45 min in a shaking incubator. After then, BM cells were washed with cold PBS to stop digestion and stained with FACS antibodies. To eliminate endothelial cells, hematopoietic cells, and erythrocytes, anti-CD31, anti-CD45, and anti-TER119 antibodies were used. Cell sorting was done with SH800 Cell Sorter (Sony Biotechnology).

For isolation of endosteal MSCs, collected bone chips were digested with Collagenase II (3 mg ml^{-1}), Dispase II (4 mg ml^{-1}), and DNase I (0.1 mg ml^{-1}) at 37 °C for 1 h 30 min in a shaking incubator. Next, bone chips were washed with α-MEM medium (10% FCS, 1% penicillin–streptomycin) three times and seeded into a 60 mm culture dish with α-MEM medium (10% FCS, 1% penicillin–streptomycin). Bone chips were cultured for 3 days at 37 °C in a 5% CO_2 incubator. After 3 days, non-adherent cells were removed and moved to a fresh medium. On the fifth culture day, adherent cells migrated from the digested bone chips were harvested using 0.25% (wt/vol) trypsin and reseeded into a culture plate. The cells were serially passaged until ten passages. All experiment was performed with cells in 3–8 passages. For EZH2 inhibition, cells were cultured with GSK126 (Selleckchem, S7061) and GSK343 (Selleckchem, S7164) or DMSO control for 24 h at 37 °C in a 5% CO_2 incubator.

RNA extraction and real-time quantitative PCR

Total RNA was purified from cells with TRIzol reagent (Molecular Research Center, Inc.) according to the manufacturer's instructions. Reverse transcription of the equal amount of isolated RNA was performed using a QuantiTect Reverse Transcription Kit (Qiagen). Real-time quantitative PCR was conducted with SYBR master mix using Step One Plus (Applied Biosystems). *Actb* was used to normalize gene expression. The primers used in this study are listed in Table S1.

In vitro co-culture of LSKs with endosteal MSCs

Endosteal MSCs (1×10^4 cells/well) were plated into a 24 well plate with α-MEM medium (10% FCS, 1% penicillin–streptomycin) and cultured at 37 °C in a 5% CO_2 incubator until it reached ~60% confluency. CD45.1$^+$ congenic-derived 2000 LSK cells (Lin$^-$Sca1$^+$cKit$^+$) were seeded into a monolayer of endosteal MSCs supplemented with mFLT-3L (30 ng/ml, R&D System), mIL-7 (30 ng/ml, R&D System), mSCF (25 ng/ml, R&D System). After 5 days, half of the cultured medium was carefully moved to a fresh α-MEM medium supplemented with mFLT-3L (30 ng/ml), mIL-7 (30 ng/ml), mSCF (25 ng/ml). On the tenth culture day, non-adherent cells were harvested and stained with anti-B220, anti-CD11b, anti-CD11c, anti-GR1 antibodies for flow cytometric analysis. For G-CSF neutralizing, anti-G-CSF antibody (1 μg/ml, R&D System) or control IgG (R&D System) was supplemented on the first and five culture day.

For collection of MSC conditioned medium, endosteal MSCs (1×10^5 cells/well) were plated into a 100 mm culture dish with α-MEM medium (10% FCS, 1% penicillin–streptomycin) and cultured at 37 °C in a 5% CO_2 incubator until it reached approximately 70 ~ 80% confluency. Then MSCs were washed three times using PBS, and cultured with fresh α-MEM medium. After 24 h of incubation, MSC conditioned medium was collected and centrifuged at 3000 rpm for 10 min to remove cell debris, and filtered through 0.45 μm filters. Fresh MSC conditioned medium was always used in each experiment.

RNA-sequencing and data analysis

Total RNA from endosteal MSCs of *Bap1* cKO ($n = 3$) and control ($n = 3$) mice were extracted using TRIzol reagent (Molecular Research Center) according to the manufacturer's instructions. The libraries were prepared for 151 bp paired-end sequencing using TruSeq stranded mRNA Sample Preparation Kit (Illumina). These cDNA libraries were qualified with the Agilent 2100 BioAnalyzer (Agilent) and quantified with the KAPA library quantification kit (Kapa Biosystems) according to the manufacturer's library protocol. Sequencing was performed as paired-end (2×151 bp) using Illumina NovaSeq 6000 (Illumina). The adapter sequences and the ends of the reads less than Phred quality score 20 were removed, and simultaneously the reads < 50 bp were removed by using cutadapt v.2.8 [57]. Filtered reads were mapped to the *Mus musculus* reference genome (GRCm38) using the aligner STAR v.2.7.1a [58]. Gene expression estimation was conducted by RSEM v.1.3.1 [59]. To normalize sequencing depth among samples, FPKM and TPM values were calculated. Differentially expressed genes (DEGs) were identified using the R package called TCC v.1.26.0 based on the estimated read counts [60]. The DEGs were identified based on the *p*-value threshold < 0.05 for correcting errors caused by multiple-testing [61] and filtered by 2-fold up- or downregulated genes in *Bap1* cKO sample compared to control sample. Gene set enrichment analysis performed based on Gene Ontology (www.geneontology.org/).

Western blotting

Cells were lysed with EzRIPA lysis buffer (150 mM NaCl, 0.1% SDS, 1% NP-40, 0.5% Deoxycholic acid, 20 mM HEPES pH7.5, ATTO) supplemented with a protease inhibitor cocktail (Roche). For isolation of nuclear extracts, cells were washed and lysed using NE-PER Nuclear and Cytoplasmic Extraction Reagents (Thermo Scientific) according to the manufacturer's instructions. Cell lysates were separated by SDS-PAGE gel electrophoresis, and transferred to Immobilon PVDF transfer membranes (Merck). Immunoblotting was performed using anti-BAP1 (sc-28236), anti-Lamin A/C (Cell signaling), anti-ubiquityl-H2AK119 (Cell signaling), anti-trimethyl-H3K27 (Cell signaling), anti-H2A (Abcam), and anti-H3 (Abcam) antibodies. Original western blots were included in the Supplementary Material.

Chromatin immunoprecipitation (ChIP) assay

To cross-link DNA to histones, 10^6 endosteal MSC were harvested and incubated with a 1% formaldehyde solution for 10 min at 37 °C on a rocker. After fixation, the cells were lysed with EzRIPA lysis buffer (150 mM NaCl, 0.1% SDS, 1% NP-40, 0.5% Deoxycholic acid, 20 mM HEPES pH7.5, ATTO) supplemented with a protease inhibitor and sonicated using a Bioruptor to make an average of 300 ~ 500 bp length. For pre-clearing, the sonicated cell supernatants were diluted with ChIP dilution buffer (0.01% SDS, 1.1% Triton X-100, 1.2 mM EDTA, 16.7 mM Tris-HCl pH 8.1, 167 mM NaCl) and incubated with Protein A Agarose/Salmon Sperm DNA (Millipore) for 30 min at 4 °C on a rocker. Then, the samples were incubated with isotype control anti-rabbit IgG (Upstate), anti-ubiquityl-H2AK119 (Cell signaling), anti-trimethyl-H3K27 (Cell signaling), anti-acetyl-H3K27 (Abcam), anti-trimethyl-H3K4 (Abcam) antibodies overnight at 4 °C on a rocker. The beads were consecutively washed twice with a low salt buffer (0.1% SDS, 1% Triton X-100, 2 mM EDTA, 20 mM Tris-HCl pH 8.1, 150 mM NaCl), a high-salt buffer (0.1% SDS, 1% Triton X-100, 2 mM EDTA, 20 mM Tris-HCl pH 8.1, 500 mM NaCl), LiCl washing buffer (0.25 M LiCl, 1% NP-40, 1% deoxycholate, 1 mM EDTA, 10 mM Tris-HCl pH 8.1) and TE buffer (10 mM Tris pH 8, 1 mM EDTA). After washing of the beads, DNA-histone complexes were eluted with elution buffer (1% SDS, 0.1 M $NaHCO_3$) and were incubated with 5 M NaCl for 4 h at 65 °C to reverse DNA-histone cross-linking. Then, DNA was purified using QIAquick Spin Kit (Qiagen). Purified DNA was analyzed by real-time quantitative PCR using Step One Plus (Applied Biosystems). The primers used in this study are listed in Table S2.

ChIP sequencing (ChIP-seq) and data analysis

Endosteal MSCs were isolated from *Bap1* cKO ($n = 2$) and control ($n = 2$) mice, and then incubated with anti-ubiquityl-H2AK119, anti-trimethyl-H3K27, anti-acetyl-H3K27, or anti-trimethyl-H3K4 antibodies. DNA samples for ChIP-seq were prepared from MSCs in the above conditions as described in the ChIP assay. The ChIP-seq libraries were prepared using TruSeq DNA Sample Prep Kit (Illumina), and then sequenced using the NovaSeq 6000 (Illumina). For the resulting 101-bp paired-end read sequences, adapter sequences were trimmed using cutadapt v.1.18 [57]. Remaining reads were then aligned to the *Mus musculus* reference genome (GRCm38) using Bowtie2 v.2.4.5 [62] with the default parameters. PCR or optical duplicate reads, multi-mapped reads, and the reads aligned with mapping quality (MAPQ) < 5 were filtered out using SAMtools v.1.9 [63] and Picard v.2.25.5 (https://broadinstitute.github.io/picard/). Next, the genomic region between TSS−5kb and TSS+5 kb was binned into 50-bp bins, and the number of reads in each bin was counted using the coverage

tool from BEDtools v.2.30.0 [64] with the default parameters. The read counts were then converted to counts per million (CPM) based on the library size.

Statistical analysis

The statistical significance was performed by two-tailed Student's *t*-test using Prism 8 (GraphPad). The *P*-values are indicated in each figure legend by asterisks (*$p < 0.05$, **$p < 0.01$, ***$p < 0.001$, ****$p < 0.0001$) and n.s (non-significant, $p > 0.05$).

DATA AVAILABILITY

The raw RNA-seq and ChIP-seq data generated in this study have been deposited in NCBI Gene Expression Omnibus database (accession numbers of GSE198823 for RNA-seq data and GSE198649 for ChIP-seq data).

REFERENCES

1. Wilson A, Trumpp A. Bone-marrow haematopoietic-stem-cell niches. Nat Rev Immunol. 2006;6:93–106.
2. Pinho S, Frenette PS. Haematopoietic stem cell activity and interactions with the niche. Nat Rev Mol Cell Biol. 2019;20:303–20.
3. Morrison SJ, Scadden DT. The bone marrow niche for haematopoietic stem cells. Nature. 2014;505:327–34.
4. Wang LD, Wagers AJ. Dynamic niches in the origination and differentiation of haematopoietic stem cells. Nat Rev Mol Cell Biol. 2011;12:643–55.
5. Tikhonova AN, Dolgalev I, Hu H, Sivaraj KK, Hoxha E, Cuesta-Dominguez A, et al. The bone marrow microenvironment at single-cell resolution. Nature. 2019;569:222–8.
6. Baryawno N, Przybylski D, Kowalczyk MS, Kfoury Y, Severe N, Gustafsson K, et al. A cellular taxonomy of the bone marrow stroma in homeostasis and leukemia. Cell. 2019;177:1915–32.
7. Scheuermann JC, de Ayala Alonso AG, Oktaba K, Ly-Hartig N, McGinty RK, Fraterman S, et al. Histone H2A deubiquitinase activity of the Polycomb repressive complex PR-DUB. Nature. 2010;465:243–7.
8. Campagne A, Lee MK, Zielinski D, Michaud A, Le Corre S, Dingli F, et al. BAP1 complex promotes transcription by opposing PRC1-mediated H2A ubiquitylation. Nat Commun. 2019;10:348.
9. Carbone M, Yang H, Pass HI, Krausz T, Testa JR, Gaudino G. BAP1 and cancer. Nat Rev Cancer. 2013;13:153–9.
10. Testa JR, Cheung M, Pei J, Below JE, Tan Y, Sementino E, et al. Germline BAP1 mutations predispose to malignant mesothelioma. Nat Genet. 2011;43:1022–5.
11. Carbone M, Harbour JW, Brugarolas J, Bononi A, Pagano I, Dey A, et al. Biological mechanisms and clinical significance of BAP1 mutations in human cancer. Cancer Disco. 2020;10:1103–20.
12. Carbone M, Adusumilli PS, Alexander HR Jr., Baas P, Bardelli F, Bononi A, et al. Mesothelioma: Scientific clues for prevention, diagnosis, and therapy. CA Cancer J Clin. 2019;69:402–29.
13. Harbour JW, Onken MD, Roberson ED, Duan S, Cao L, Worley LA, et al. Frequent mutation of BAP1 in metastasizing uveal melanomas. Science. 2010;330:1410–3.
14. Kadariya Y, Cheung M, Xu J, Pei J, Sementino E, Menges CW, et al. Bap1 is a bona fide tumor suppressor: genetic evidence from mouse models carrying heterozygous germline Bap1 mutations. Cancer Res. 2016;76:2836–44.
15. Masclef L, Ahmed O, Estavoyer B, Larrivee B, Labrecque N, Nijnik A, et al. Roles and mechanisms of BAP1 deubiquitinase in tumor suppression. Cell Death Differ. 2021;28:606–25.
16. Machida YJ, Machida Y, Vashisht AA, Wohlschlegel JA, Dutta A. The deubiquitinating enzyme BAP1 regulates cell growth via interaction with HCF-1. J Biol Chem. 2009;284:34179–88.
17. Misaghi S, Ottosen S, Izrael-Tomasevic A, Arnott D, Lamkanfi M, Lee J, et al. Association of C-terminal ubiquitin hydrolase BRCA1-associated protein 1 with cell cycle regulator host cell factor 1. Mol Cell Biol. 2009;29:2181–92.
18. Ji Z, Mohammed H, Webber A, Ridsdale J, Han N, Carroll JS, et al. The forkhead transcription factor FOXK2 acts as a chromatin targeting factor for the BAP1-containing histone deubiquitinase complex. Nucleic Acids Res. 2014;42:6232–42.
19. Yu H, Mashtalir N, Daou S, Hammond-Martel I, Ross J, Sui G, et al. The ubiquitin carboxyl hydrolase BAP1 forms a ternary complex with YY1 and HCF-1 and is a critical regulator of gene expression. Mol Cell Biol. 2010;30:5071–85.
20. Dey A, Seshasayee D, Noubade R, French DM, Liu J, Chaurushiya MS, et al. Loss of the tumor suppressor BAP1 causes myeloid transformation. Science. 2012;337:1541–6.
21. Ruan HB, Han X, Li MD, Singh JP, Qian K, Azarhoush S, et al. O-GlcNAc transferase/host cell factor C1 complex regulates gluconeogenesis by modulating PGC-1alpha stability. Cell Metab. 2012;16:226–37.
22. Daou S, Hammond-Martel I, Mashtalir N, Barbour H, Gagnon J, Iannantuono NV, et al. The BAP1/ASXL2 histone H2A deubiquitinase complex regulates cell proliferation and is disrupted in cancer. J Biol Chem. 2015;290:28643–63.
23. Bononi A, Giorgi C, Patergnani S, Larson D, Verbruggen K, Tanji M, et al. BAP1 regulates IP3R3-mediated Ca^{2+} flux to mitochondria suppressing cell transformation. Nature. 2017;546:549–53.
24. Arenzana TL, Lianoglou S, Seki A, Eidenschenk C, Cheung T, Seshasayee D, et al. Tumor suppressor BAP1 is essential for thymic development and proliferative responses of T lymphocytes. Sci Immunol. 2018;3:eaal1953.
25. LaFave LM, Beguelin W, Koche R, Teater M, Spitzer B, Chramiec A, et al. Loss of BAP1 function leads to EZH2-dependent transformation. Nat Med. 2015;21:1344–9.
26. Lin YH, Liang Y, Wang H, Tung LT, Forster M, Subramani PG, et al. Regulation of B lymphocyte development by histone H2A deubiquitinase BAP1. Front Immunol. 2021;12:626418.
27. Logan M, Martin JF, Nagy A, Lobe C, Olson EN, Tabin CJ. Expression of Cre Recombinase in the developing mouse limb bud driven by a Prxl enhancer. Genesis. 2002;33:77–80.
28. Greenbaum A, Hsu YM, Day RB, Schuettpelz LG, Christopher MJ, Borgerding JN, et al. CXCL12 in early mesenchymal progenitors is required for haematopoietic stem-cell maintenance. Nature. 2013;495:227–30.
29. Zhou BO, Yue R, Murphy MM, Peyer JG, Morrison SJ. Leptin-receptor-expressing mesenchymal stromal cells represent the main source of bone formed by adult bone marrow. Cell Stem Cell. 2014;15:154–68.
30. Yue R, Zhou BO, Shimada IS, Zhao Z, Morrison SJ. Leptin receptor promotes adipogenesis and reduces osteogenesis by regulating mesenchymal stromal cells in adult bone marrow. Cell Stem Cell. 2016;18:782–96.
31. Cordeiro Gomes A, Hara T, Lim VY, Herndler-Brandstetter D, Nevius E, Sugiyama T, et al. Hematopoietic stem cell niches produce lineage-instructive signals to control multipotent progenitor differentiation. Immunity. 2016;45:1219–31.
32. Charbord P, Pouget C, Binder H, Dumont F, Stik G, Levy P, et al. A systems biology approach for defining the molecular framework of the hematopoietic stem cell niche. Cell Stem Cell. 2014;15:376–91.
33. Wang L, Zhao Z, Ozark PA, Fantini D, Marshall SA, Rendleman EJ, et al. Resetting the epigenetic balance of Polycomb and COMPASS function at enhancers for cancer therapy. Nat Med. 2018;24:758–69.
34. Boyer LA, Plath K, Zeitlinger J, Brambrink T, Medeiros LA, Lee TI, et al. Polycomb complexes repress developmental regulators in murine embryonic stem cells. Nature. 2006;441:349–53.
35. Wang H, Wang L, Erdjument-Bromage H, Vidal M, Tempst P, Jones RS, et al. Role of histone H2A ubiquitination in Polycomb silencing. Nature. 2004;431:873–8.
36. Bernstein BE, Humphrey EL, Erlich RL, Schneider R, Bouman P, Liu JS, et al. Methylation of histone H3 Lys 4 in coding regions of active genes. Proc Natl Acad Sci USA. 2002;99:8695–8700.
37. Creyghton MP, Cheng AW, Welstead GG, Kooistra T, Carey BW, Steine EJ, et al. Histone H3K27ac separates active from poised enhancers and predicts developmental state. Proc Natl Acad Sci USA. 2010;107:21931–6.
38. Margueron R, Reinberg D. The Polycomb complex PRC2 and its mark in life. Nature. 2011;469:343–9.
39. Matthias P, Rolink AG. Transcriptional networks in developing and mature B cells. Nat Rev Immunol. 2005;5:497–508.
40. Loder F, Mutschler B, Ray RJ, Paige CJ, Sideras P, Torres R, et al. B cell development in the spleen takes place in discrete steps and is determined by the quality of B cell receptor-derived signals. J Exp Med. 1999;190:75–89.
41. Ding L, Morrison SJ. Haematopoietic stem cells and early lymphoid progenitors occupy distinct bone marrow niches. Nature. 2013;495:231–5.
42. Asada N, Kunisaki Y, Pierce H, Wang Z, Fernandez NF, Birbrair A, et al. Differential cytokine contributions of perivascular haematopoietic stem cell niches. Nat Cell Biol. 2017;19:214–23.
43. Ding L, Saunders TL, Enikolopov G, Morrison SJ. Endothelial and perivascular cells maintain haematopoietic stem cells. Nature. 2012;481:457–62.
44. Koni PA, Joshi SK, Temann U-A, Olson D, Burkly L, Flavell RA. Conditional vascular cell adhesion molecule 1 deletion in mice: impaired lymphocyte migration to bone marrow. J Exp Med. 2001;193:741–54.
45. Scott LM, Priestley GV, Papayannopoulou T. Deletion of alpha4 integrins from adult hematopoietic cells reveals roles in homeostasis, regeneration, and homing. Mol Cell Biol. 2003;23:9349–60.
46. Zhou BO, Ding L, Morrison SJ. Hematopoietic stem and progenitor cells regulate the regeneration of their niche by secreting Angiopoietin-1. Elife. 2015;4:e05521.
47. Arai F, Hirao A, Ohmura M, Sato H, Matsuoka S, Takubo K, et al. Tie2/angiopoietin-1 signaling regulates hematopoietic stem cell quiescence in the bone marrow niche. Cell. 2004;118:149–61.
48. Nilsson SK, Johnston HM, Whitty GA, Williams B, Webb RJ, Denhardt DT, et al. Osteopontin, a key component of the hematopoietic stem cell niche and regulator of primitive hematopoietic progenitor cells. Blood. 2005;106:1232–9.

49. Oswald J, Steudel C, Salchert K, Joergensen B, Thiede C, Ehninger G, et al. Gene-expression profiling of CD34^{+} hematopoietic cells expanded in a collagen I matrix. Stem Cells. 2006;24:494–500.
50. Dao MA, Hashino K, Kato I, Nolta JA. Adhesion to fibronectin maintains regenerative capacity during ex vivo culture and transduction of human hematopoietic stem and progenitor cells. Blood. 1998;92:4612–21.
51. Soehnlein O, Steffens S, Hidalgo A, Weber C. Neutrophils as protagonists and targets in chronic inflammation. Nat Rev Immunol. 2017;17:248–61.
52. Bendall LJ, Bradstock KF. G-CSF: From granulopoietic stimulant to bone marrow stem cell mobilizing agent. Cytokine Growth Factor Rev. 2014;25:355–67.
53. Aranda S, Mas G, Di Croce L. Regulation of gene transcription by Polycomb proteins. Sci Adv. 2015;1:e1500737.
54. Zhang Y, Shi J, Liu X, Feng L, Gong Z, Koppula P, et al. BAP1 links metabolic regulation of ferroptosis to tumour suppression. Nat Cell Biol. 2018;20:1181–92.
55. Costa LA, Eiro N, Fraile M, Gonzalez LO, Saa J, Garcia-Portabella P, et al. Functional heterogeneity of mesenchymal stem cells from natural niches to culture conditions: implications for further clinical uses. Cell Mol Life Sci. 2021;78:447–67.
56. Skarnes WC, Rosen B, West AP, Koutsourakis M, Bushell W, Iyer V, et al. A conditional knockout resource for the genome-wide study of mouse gene function. Nature. 2011;474:337–42.
57. Martin M. Cutadapt removes adapter sequences from high-throughput sequencing reads. EMBnet J. 2011;17:10–12.
58. Dobin A, Davis CA, Schlesinger F, Drenkow J, Zaleski C, Jha S, et al. STAR: ultrafast universal RNA-seq aligner. Bioinformatics. 2013;29:15–21.
59. Li B, Dewey CN. RSEM: accurate transcript quantification from RNA-Seq data with or without a reference genome. BMC Bioinforma. 2011;12:1–16.
60. Sun J, Nishiyama T, Shimizu K, Kadota K. TCC: an R package for comparing tag count data with robust normalization strategies. BMC Bioinforma. 2013;14:1–14.
61. Benjamini Y, Hochberg Y. Controlling the false discovery rate: a practical and powerful approach to multiple testing. J R Stat Soc B. 1995;57:289–300.
62. Langmead B, Salzberg SL. Fast gapped-read alignment with Bowtie 2. Nat Methods. 2012;9:357–9.
63. Li H, Handsaker B, Wysoker A, Fennell T, Ruan J, Homer N, et al. The sequence alignment/map format and SAMtools. Bioinformatics. 2009;25:2078–9.
64. Quinlan AR, Hall IM. BEDTools: a flexible suite of utilities for comparing genomic features. Bioinformatics. 2010;26:841–2.

ACKNOWLEDGEMENTS

We thank members of our laboratories for providing reagents and helpful advice. We thank Hyeong-In Ham for assistance with the manuscript preparation.

AUTHOR CONTRIBUTIONS

JJ designed and performed experiments. IJ, JHK., SJ, HM, BK, JN performed the experiments. DYH and DH analyzed the ChIP-seq data. SJU provided critical materials. RHS and MK conceived and supervised the study. JJ, MK, and RHS wrote and edited the manuscript. All authors reviewed and approved the manuscript.

FUNDING

This work was supported in part by the National Research Foundation of Korea (NRF-2021R1A2B5B03002202), Korea Mouse Phenotyping Project (NRF-2014M3A9D5 A01073789) of the Ministry of Science, Information and Communication Technology, and Future Planning through the National Research Foundation (to RHS); and the National Research Foundation of Korea (NRF-2018R1A6A1A03025810), the Research Fund of UNIST (1.220023.01) (to MK).

COMPETING INTERESTS

The authors declare no competing interests.

ETHICS

All animal procedures were approved by and conducted according to the Institutional Animal Care and Use Committee (IACUC) at Seoul National University.

ADDITIONAL INFORMATION

Supplementary information The online version contains supplementary material available at https://doi.org/10.1038/s41418-022-01006-y.

Correspondence and requests for materials should be addressed to Myunggon Ko or Rho Hyun Seong.